Supporting information

In Situ Insight into Thermally-Induced Reversible Transitions of Crystal Structure and Photoluminescence Properties in Cu_2Te Nanoplate

Yanan Zhang,[a] Zhi Zhang,*[a] Weifeng Liu,[a] Yifan Zheng,[a] Yonghui Wu,[a] Jun Su,[a] Nishuang Liu[a] and Yihua Gao [a]

[a]School of Physics & Wuhan National Laboratory for Optoelectronics (WNLO), Huazhong University of Science and Technology (HUST), Luoyu Road 1037, Wuhan 430074, P. R. China

*Address correspondence to: zzhang@hust.edu.cn

The crystal structure of Cu_2Te at room temperature was investigated by XRD and all the diffraction peaks in the XRD pattern (Fig.S1a) can be indexed to the hexagonal *α*-Cu_2Te with the space group of P3m1 and lattice parameters of a = b = 8.367 Å, c = 21.627Å (PDF 57-0477). Moreover, Cu_2Te shows no other diffraction peaks in its XRD pattern, suggesting its high purity. The chemical composition of Cu_2Te was studied by the quantitative analysis of EDS spectrum (Fig.S1b) in TEM. It can be seen that the atom ratio of Cu and Te elements in the sample is close to 2:1.

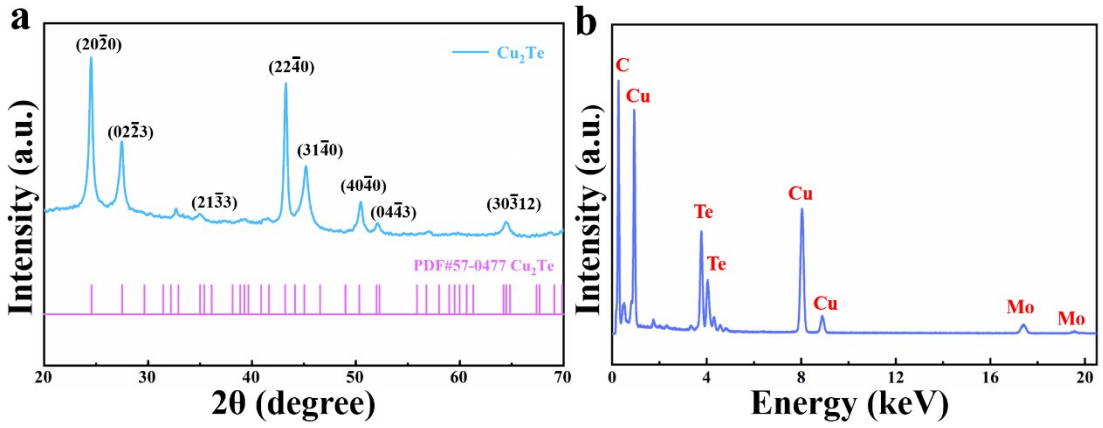

Fig.S1 (a) XRD pattern of Cu_2Te nanoplate. Sky blue line: experimental XRD pattern at room temperature; Pink line: standard PDF card 57-0477. (b) Spot EDS spectrum of Cu_2Te nanoplate.

The morphology, crystallinity and microstructure of Cu_2Te were investigated by TEM. Fig.S2a shows the bright-filed TEM image of a typical Cu_2Te, in which well-defined facets can be clearly observed in the nanoplate. Selected area electron diffraction (SAED) was used to determine the crystal structure and crystallinity of Cu_2Te nanoplate and Fig.S2b shows such a SAED pattern taken from the [0001] zone axis. Detailed analysis on the SAED pattern indicates that the Cu_2Te nanoplate crystallizes in single crystalline and hexagonal structure with the space group of P3m1 (PDF 57-0477, α-Cu_2Te). Based on the SAED pattern, the orientation and facets of Cu_2Te nanoplate can be determined, as labeled in Fig.S2a. In addition, the high-resolution TEM image was collected and displayed in Fig.S2c, in which the $(\bar{1}100)$ and $(01\bar{1}0)$ planes can be clearly resolved. The atomic configuration of α-Cu_2Te projected along the [0001] direction is shown in Fig.S2d, from which the atomic arrangement of $(\bar{1}100)$ and $(01\bar{1}0)$ planes can be distinguished, respectively. To further confirm the crystal structure of α-Cu_2Te, the SAED pattern simulation was performed based on cif file from Crystallography Open Database using the Crystal Maker software. Fig.S2e shows the simulated SAED pattern along the [0001] zone axis. It can be seen that the experimental and simulated SAED patterns are consistent. The atomic structure of α-Cu_2Te is illustrated in Fig.S2f in which large d-spacing along the c-axis can be seen. The EDS mappings were carried out to reveal the elemental distribution in α-Cu_2Te, and the results in Fig.S2g suggest the uniform distribution of Cu and Te elements in the sample.

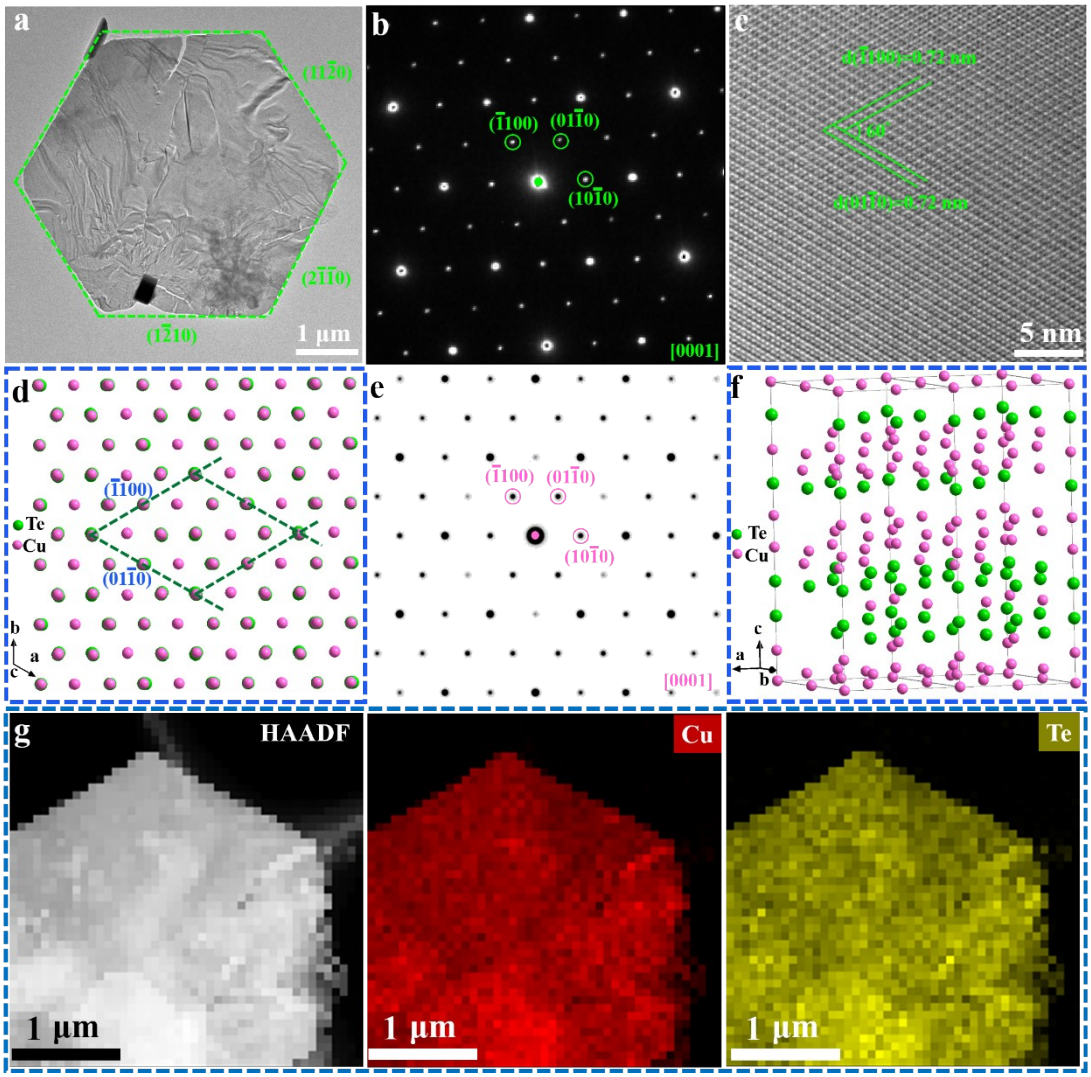

Fig.S2 (a) Bright-filed TEM image of Cu_2Te nanoplate. (b) SAED pattern taken from [0001] zone axis. (c) High-resolution TEM image of Cu_2Te nanoplate. (d) Crystal structure of Cu_2Te viewed along [0001] direction. (e) Simulated SAED pattern of Cu_2Te along [0001] zine axis. (f) Atom structure of Cu_2Te with the space group of P3m1 (PDF 57-0477, α-Cu_2Te). (g) EDS elemental mappings of Cu_2Te nanoplate.

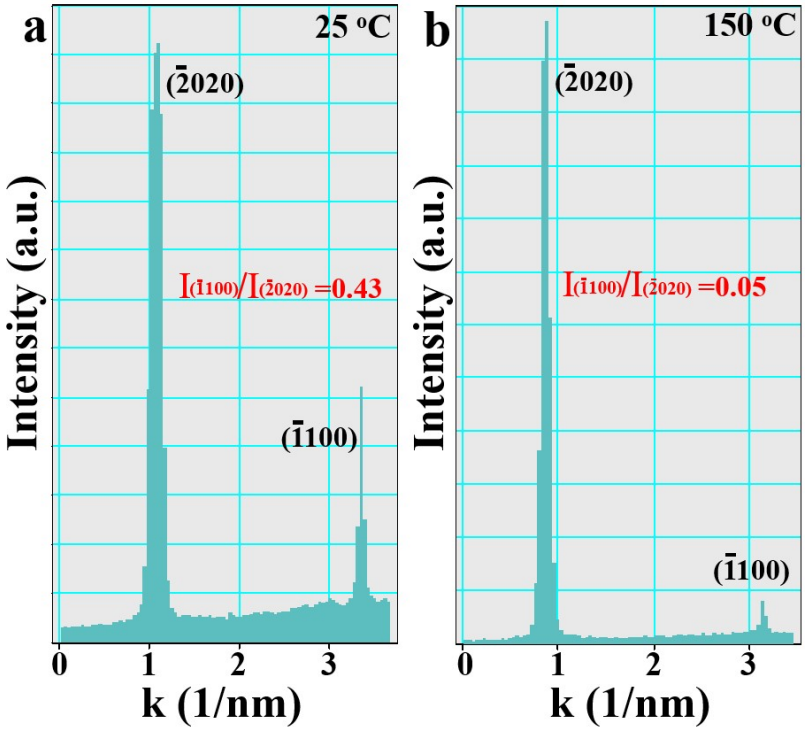

Fig.S3 Intensity profile of $(\bar{1}100)$ and $(\bar{2}020)$ diffraction spots from Fig.1a-b.

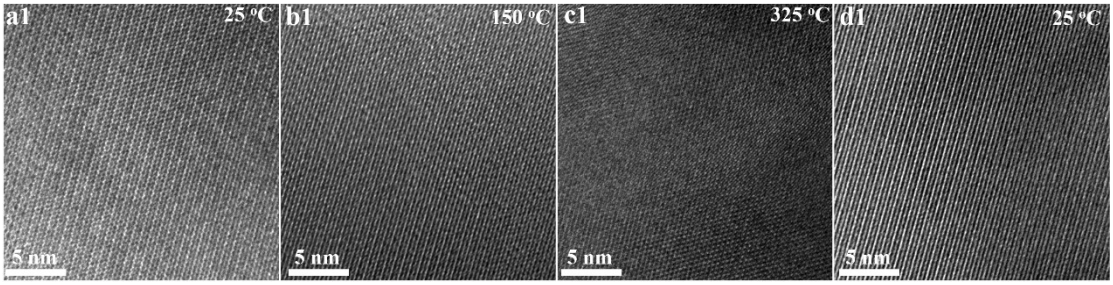

Fig.S4 The high-resolution TEM images shown in Figure 2.

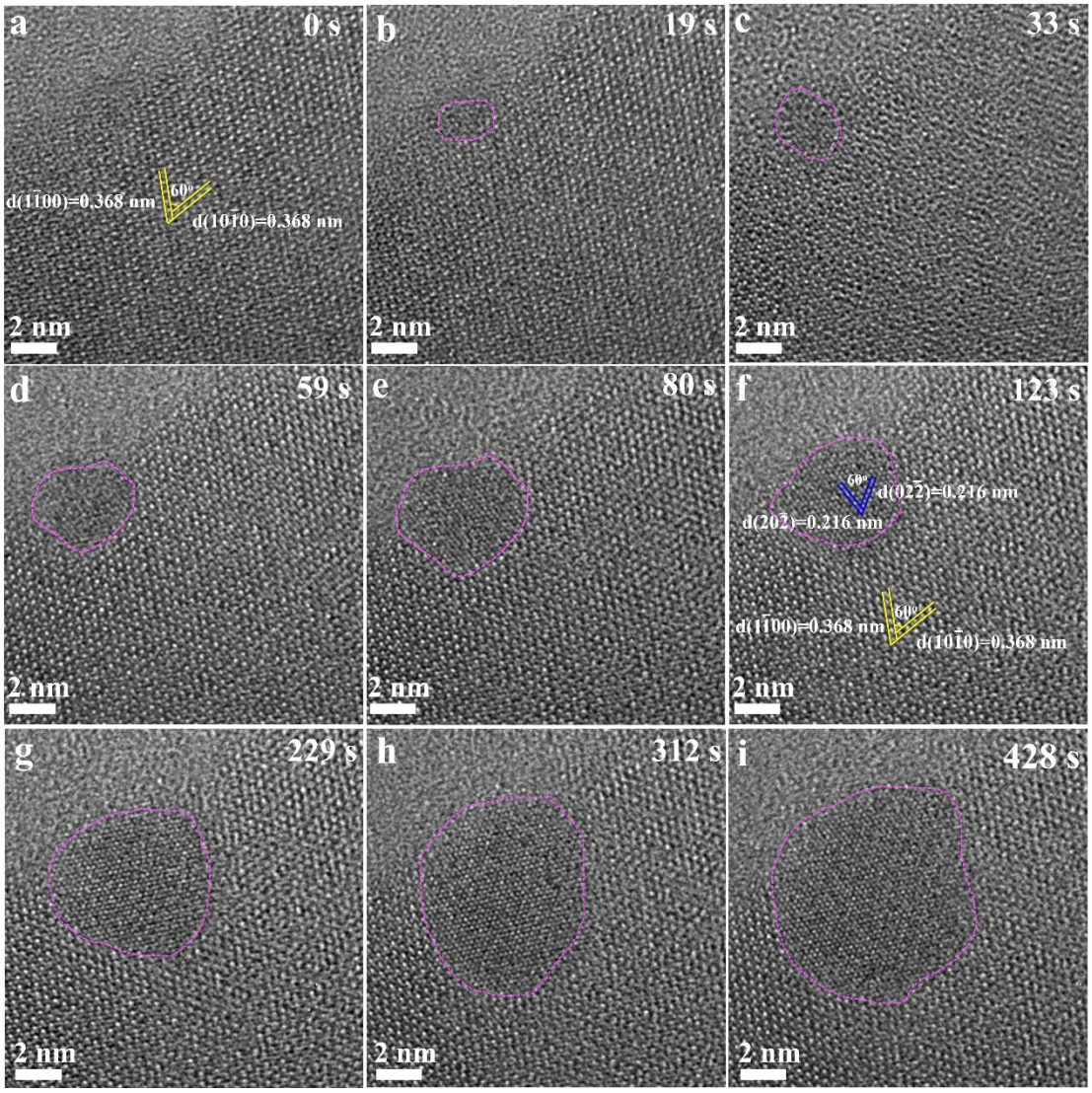

Fig.S5 The structural evolution of Cu_2Te nanoplate at elevated temperature of 575 °C. (a-i) Time-resolved high-resolution TEM images series at (a) 0 s, (b) 19 s, (c) 33 s, (d) 59 s, (e) 80 s, (f) 123 s, (g) 229 s, (h) 312 s, (i) 428 s.

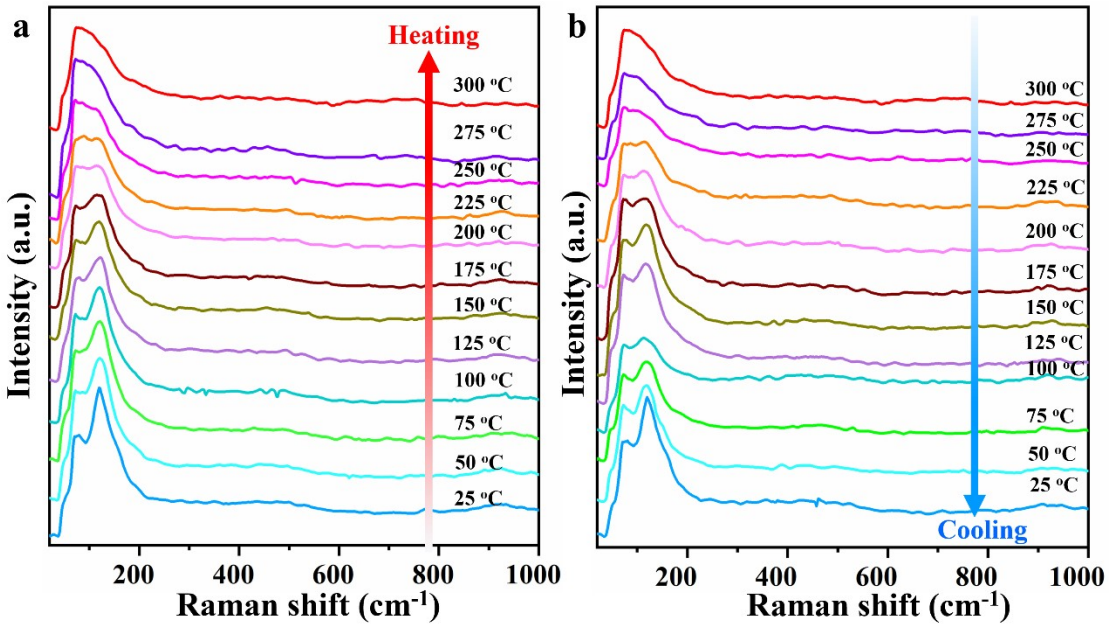

Fig.S6 (a) Temperature-dependent Raman spectra acquired in the frequency range from 20 to 1000 cm^{-1} during the heating process. (b) Temperature-dependent Raman spectra acquired in the frequency range from 20 to 1000 cm^{-1} during the cooling process.

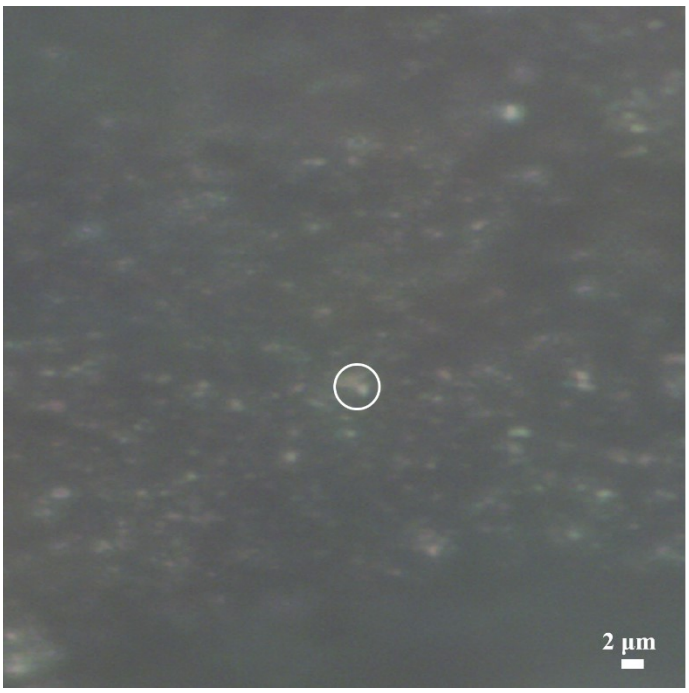

Fig.S7 Optical image of Cu_2Te after laser irradiation in Raman test.

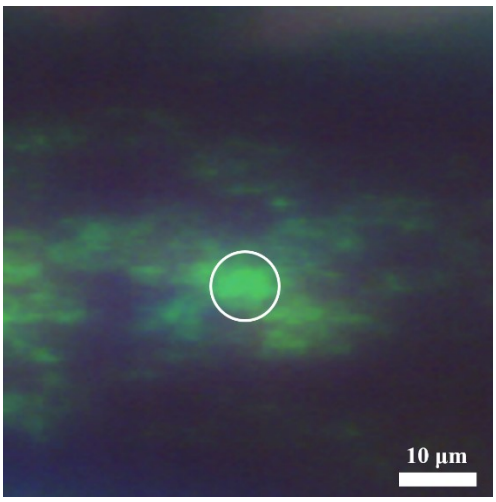

Fig.S8 Optical image of Cu_2Te nanoplate under irradiation by a focused laser with a wavelength of 325 nm and an intensity of 0.3 mW.

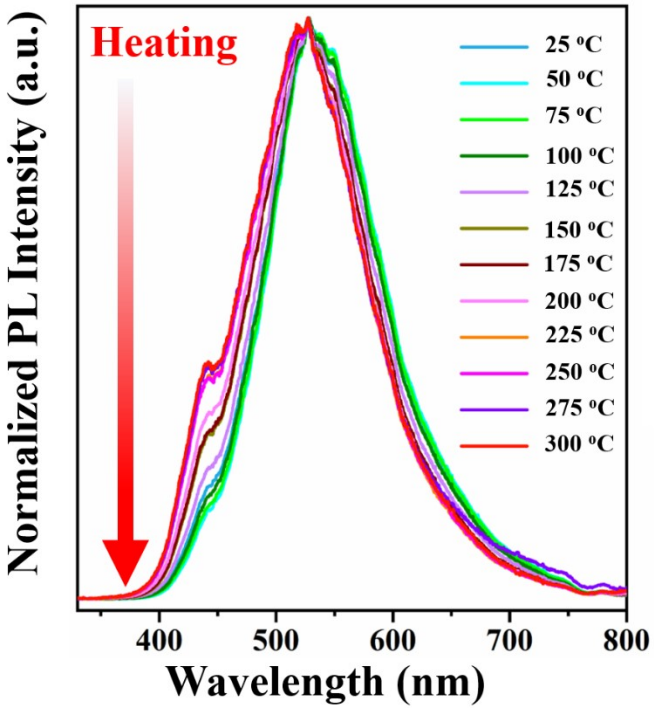

Fig.S9 Temperature-dependent normalized PL spectra of Cu_2Te nanoplate during the heating process.

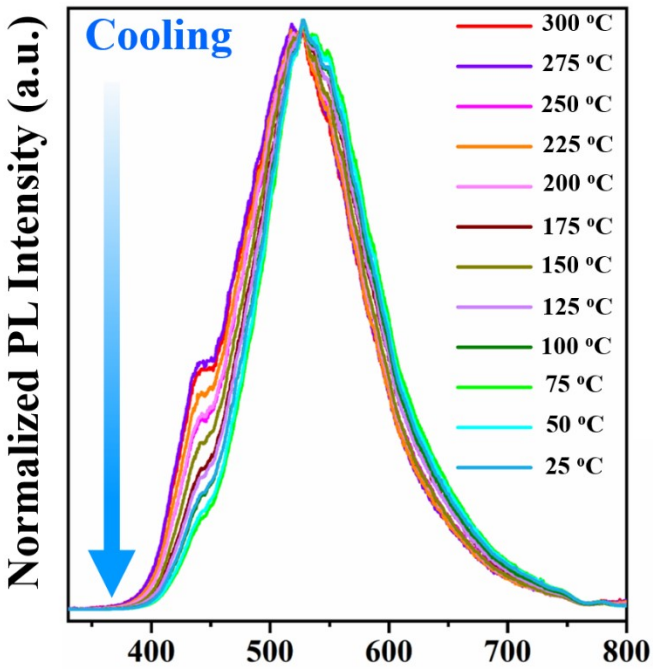

Fig.S10 Temperature-dependent normalized PL spectra of Cu_2Te nanoplate during the cooling process.

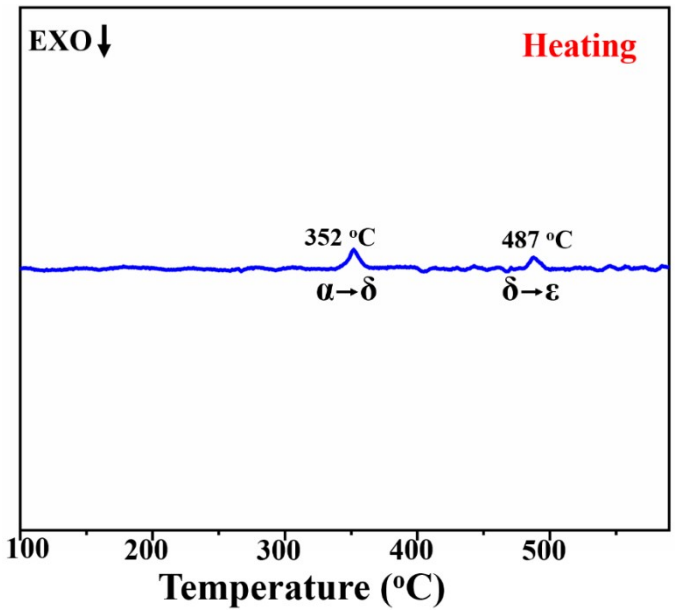

Fig. S11 DSC profiles of Cu_2Te nanoplate under flowing argon.

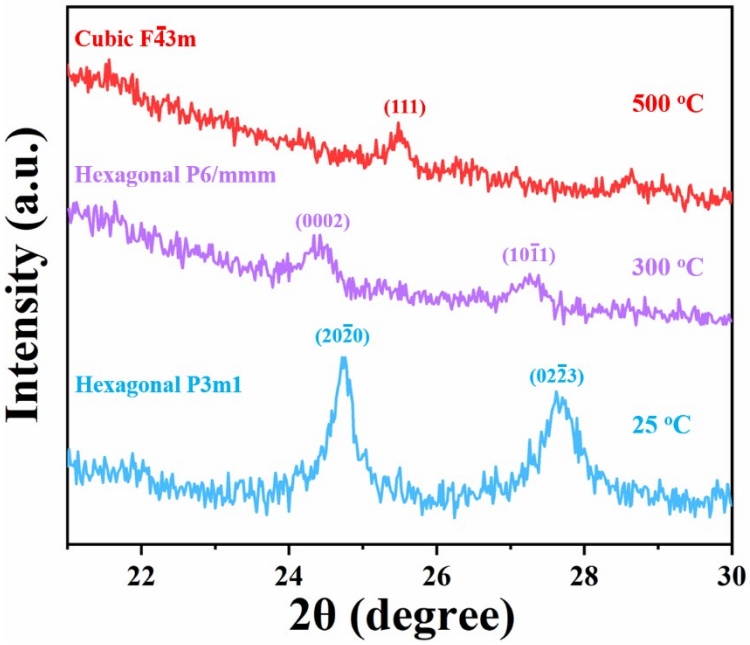

Fig. S12 HTXRD pattern of Cu_2Te nanoplate at different temperature.

Video M1. Video M1 shows the reversible phase transformation of Cu_2Te from α phase to δ phase at the cycling heating temperatures range from 25 °C-325 °C-25 °C. The video is presented at 80 times actual speed.

Video M2. Video M2 shows the structural evolution of Cu_2Te nanoplate at elevated temperature of 575 °C. The image of Fig.3 corresponds to a frame captured from this video. The video is presented at 16 times actual speed.